Impurity spin relaxation in $S=\frac{1}{2}$ XX chains

Joachim Stolze and Michael Vogel
Institut für Physik, Universität Dortmund, D-44221 Dortmund, Germany
(Received 20 May 1999; revised manuscript received 13 August 1999)

Dynamic autocorrelations $\langle S_i^\alpha(t)S_i^\alpha\rangle$ $(\alpha=x,z)$ of an isolated impurity spin in a $S=\frac{1}{2}$ XX chain are calculated. The impurity spin, defined by a local change in the nearest-neighbor coupling, is either in the bulk or at the boundary of the open-ended chain. The exact numerical calculation of the correlations employs the Jordan-Wigner mapping from spin operators to Fermi operators; the effects of finite system size can be eliminated. Two distinct temperature regimes are observed in the long-time asymptotic behavior of the bulk correlations. At $T=0$ only power laws are present. At high T the x correlation decays exponentially (except at short times), while the z correlation still shows an asymptotic power law (different from the one at $T=0$) after an intermediate exponential phase. The boundary impurity correlations ultimately follow power laws at all T, with intermediate exponential phases at high T. The power laws for the z correlation and the boundary correlations can be derived from the impurity-induced changes in the properties of the Jordan-Wigner fermion states.

I. INTRODUCTION

The $S=\frac{1}{2}$ XX chain[1,2]

$$H=-\sum_{i=1}^{N-1} J_i(S_i^xS_{i+1}^x+S_i^yS_{i+1}^y), \tag{1.1}$$

is one of the simplest quantum many-body systems conceivable, as many of its properties can be derived from those of noninteracting lattice fermions. Its equilibrium spin pair correlation functions

$$\langle S_i^\alpha(t)S_j^\alpha\rangle=\frac{\mathrm{Tr}\, e^{-\beta H}e^{itH}S_i^\alpha e^{-itH}S_j^\alpha}{\mathrm{Tr}\, e^{-\beta H}},\alpha=x,z \tag{1.2}$$

have been the objects of intense research efforts over an extended period.[3–21] Only a few explicit analytic results are available, but several existing asymptotic results for large distances $|i-j|$ or long times t have been corroborated by numerical calculations.

For XX chains with homogeneous nearest-neighbor coupling $(J_i\equiv J)$ only three different types of asymptotic long-time behavior have been observed to date: Gaussian, exponential, and power law (often with superimposed oscillations). It is interesting to speculate whether nonuniform or random couplings might induce additional types of asymptotic behavior.

In the present paper we study the changes in autocorrelation functions $\langle S_i^\alpha(t)S_i^\alpha\rangle$ induced by a single impurity spin in an otherwise homogeneous chain. The impurity spin is located either at the boundary of the system,

$$J_1=J',\quad J_i\equiv J=1 \quad \text{for} \quad i\geqslant 2 \tag{1.3}$$

or in the bulk,

$$J_{N/2-1}=J_{N/2}=J',\quad J_i\equiv J=1 \quad \text{for all other} \quad i. \tag{1.4}$$

Equilibrium and nonequilibrium dynamics of the boundary impurity were studied early on by Tjon.[5] In the weak-coupling limit $(J'\to 0)$, Tjon obtained exponential behavior of the impurity spin autocorrelation functions. Our results (see Sec. IV) show that for finite impurity coupling J', exponential behavior occurs only in an intermediate time regime, whereas the ultimate long-time behavior is a power law.

Besides their obvious relevance in low-dimensional magnetism, impurities in spin-$\frac{1}{2}$ chains are also of interest in quantum dynamics, where two-level systems coupled to ''baths'' serve as models for quantum systems in dissipative environments.[22–24] The most popular model[23] in this field is the spin-boson model, consisting of a single spin-$\frac{1}{2}$ coupled to a (quasi-) continuum of noninteracting oscillators with a given spectral density. In a recent study[25] the oscillator bath was replaced with a bath of noninteracting spins $\frac{1}{2}$. The changes in dynamic behavior which were observed as a result of this replacement suggest further exploration of different kinds of baths. The system studied here can be considered a two-level system (the impurity spin) coupled to a bath of *interacting* two-level systems (the remainder of the XX chain). An interesting feature of this system is the fact that while the z component of the total spin is conserved, the x component is not. Thus differences are to be expected between the relaxation of the x and z components of the impurity spin.

The plan of the paper is as follows: In Sec. II we discuss the method used to calculate the dynamic correlation functions numerically. In Sec. III we present results for spin autocorrelation functions of a bulk impurity spin (and also of its neighbors) for both zero and finite T. In Sec. IV we discuss boundary impurity autocorrelation functions. Section V summarizes our findings.

II. METHOD

The open-ended N-site spin-$\frac{1}{2}$ XX chain described by the Hamiltonian (1.1) can be mapped to a Hamiltonian of noninteracting fermions,

$$\tilde{H}=-\frac{1}{2}\sum_{i=1}^{N-1} J_i(c_i^\dagger c_{i+1}+c_{i+1}^\dagger c_i) \tag{2.1}$$

by means of the Jordan-Wigner transformation[1,2] between spin and fermion operators:

$$S_i^z=c_i^\dagger c_i-\frac{1}{2}, \tag{2.2}$$

$$S_i^+=(-1)^{\sum_{k=1}^{i-1} c_k^\dagger c_k} c_i^\dagger=\prod_{k=1}^{i-1}(1-2c_k^\dagger c_k)c_i^\dagger . \tag{2.3}$$

In the homogeneous case $J_i\equiv J$, the one-particle energy eigenvalues are

$$\varepsilon_k=-J\cos k,\quad k=\frac{\nu\pi}{N+1},\quad \nu=1,\ldots,N, \tag{2.4}$$

and the eigenvectors are sinusoidal functions of the site index i. For general J_i neither eigenvalues nor eigenvectors are available analytically, however, both are easily obtained from the solution of a tridiagonal eigenvalue problem with standard numerical procedures.[26]

The spin correlation functions (1.2) are mapped to fermion correlation functions, with crucial differences between the cases $\alpha=z$ and $\alpha=x$. $\langle S_i^z(t)S_j^z\rangle$ maps to a density-density correlation function involving four Fermi operators. Due to the string of signs in Eq. (2.3), however, $\langle S_i^x(t)S_j^x\rangle$ maps to a *many-particle* correlation function involving $2(i+j-1)$ Fermi operators. Wick's theorem can be applied to expand $\langle S_i^x(t)S_j^x\rangle$ in products of elementary fermion expectation values. That expansion can be most compactly expressed as a Pfaffian[27] whose elements are sums involving the one-particle eigenvalues and eigenvectors.

In order to obtain results valid in the thermodynamic limit $N\to\infty$, finite-size effects must be identified and eliminated. As finite-size effects are known[21] to be caused by reflections of propagating excitations from the boundaries of the system, the maximum fermion group velocity [see Eq. 2.4)] can be used to estimate the time range over which a given spin correlation function (1.2) can be expected to be free of finite-size effects. That estimate can then be verified by explicit numerical calculation of equivalent correlation functions for system sizes N_0 and, say, $2N_0$.

The one-fermion eigenvalue problem for the single-impurity chain (1.3) or (1.4) (Ref. 28) may be solved analytically. The nature of the solution depends on the value of J'. For J' below a critical value J_c all states are extended and the continuous energy spectrum is given by ε_k Eq. (2.4) with J'-dependent k values. For $J'>J_c$ a pair of exponentially localized impurity states with energies $\pm\varepsilon_0$, $|\varepsilon_0|>1$, emerge from the continuum. The critical coupling strength is $J_c=1$ for the bulk impurity and $J_c=\sqrt{2}$ for the boundary impurity. Below, we occasionally refer to properties of the analytic solution in order to explain the long-time asymptotic behavior observed in the numerical results.

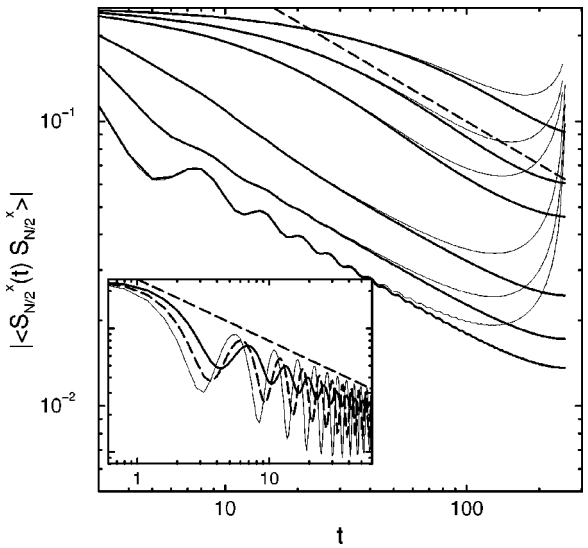

FIG. 1. Bulk impurity spin x autocorrelation function $|\langle S_{N/2}^x(t)S_{N/2}^x\rangle|$ at $T=0$. Main plot: $N=512$, impurity coupling $J'<1$. The heavy solid lines (top to bottom) correspond to $J'=0.1$, 0.15, 0.2, 0.4, 0.6, and 0.8. The dashed straight line is the $t^{-1/2}$ power law (3.1). The thin solid lines are $N=256$ data demonstrating the influence of the system size. Inset: $N=128$, $J'>1$. Shown are data for $J'=1$ (heavy solid line), $J'=1.2$ (dashed curve), and $J'=1.4$ (thin solid line). The dashed straight line is again the $t^{-1/2}$ power law (3.1).

III. BULK IMPURITY

A. $T=0$

The long-time asymptotic behavior of the $T=0$ bulk impurity spin x autocorrelation functions is difficult to obtain due to a combination of two reasons. First, this correlation is the computationally most demanding one, as large Pfaffians have to be evaluated. Second, it is also the correlation function displaying finite-size effects at the earliest times. This may be related to its particularly slow long-time asymptotic decay law[11,14,15]

$$\langle S_i^x(t)S_{i+n}^x\rangle\sim(n^2-J^2t^2)^{-1/4}\quad \text{for}\ \ T=0 \tag{3.1}$$

in the homogeneous case $J_i\equiv J$. It should be noted that the right-hand side of Eq. (3.1) is the leading term of an asymptotic expansion; its character changes from purely real (for $J^2t^2<n^2$) to complex (for $J^2t^2>n^2$). More explicit forms are Eq. (1.23) in Ref. 11 and Eqs. (59), (61) in Ref. 15.

We have calculated $\langle S_{N/2}^x(t)S_{N/2}^x\rangle$ for impurity coupling constants $0.1\leqslant J'\leqslant 4$. In all cases the asymptotic decay of the correlation function was consistent with the $t^{-1/2}$ law Eq. (3.1). With growing J' $|\langle S_{N/2}^x(t)S_{N/2}^x\rangle|$ develops oscillations of rather well-defined frequency and growing amplitude, as shown in the inset of Fig. 1. The frequency of the oscillations for $J'>1$ is proportional to the energy

$$|\varepsilon_0|=\frac{J'^2}{\sqrt{2J'^2-1}}\quad (J'>1) \tag{3.2}$$

of the localized impurity state. On the whole, the long-time asymptotic behavior of the impurity spin x autocorrelation at $T=0$ is not fundamentally changed by varying the value of J'.

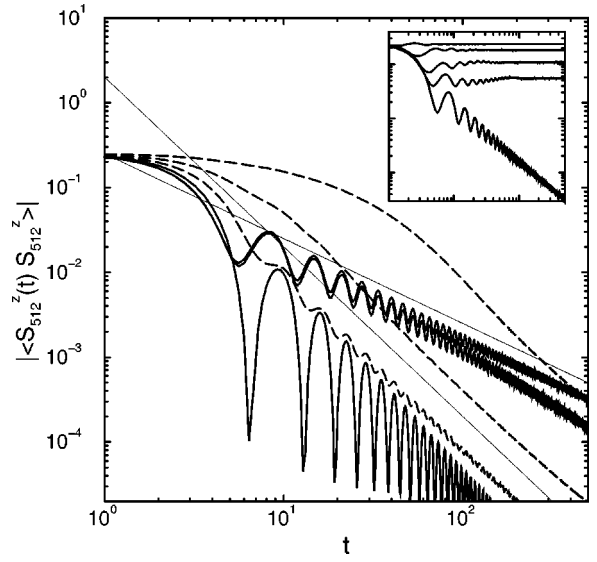

FIG. 2. Main plot: Bulk impurity spin z autocorrelation function $|\langle S^z_{N/2}(t)S^z_{N/2}\rangle|$ ($N=1024$) at $T=0$, for impurity couplings $J'=1$, 0.99, 0.8 (solid lines, top to bottom); $J'=0.6$, 0.4, 0.2 (long-dashed lines, bottom to top). The thin straight lines show the power laws t^{-1} and t^{-2}. Inset: same as main plot, for $J'=1$, 1.2, 1.4, 2,4 (bottom to top).

The impurity spin z autocorrelation, in contrast, changes significantly when J' is varied, as shown in Fig. 2. For small J' $|\langle S^z_{N/2}(t)S^z_{N/2}\rangle|$ displays a monotonic decay. Roughly at $J'=0.5$ oscillations (of well-defined and J'-independent frequency) begin to develop. For all $J'<1$ the correlation function follows an asymptotic t^{-2} law. The $J'=1$ correlation shows the t^{-1} law well known[3,4,16] for the homogeneous case. As soon as J' is further increased, the behavior changes again and the absolute value of the correlation function tends to a constant nonzero value for large times.

The changes in the asymptotics of $|\langle S^z_{N/2}(t)S^z_{N/2}\rangle|$ can be understood from the analytic solution mentioned in Sec. II. The Jordan-Wigner transformation yields, after a few simple steps

$$\langle S_i^z(t)S_i^z\rangle=\left(\sum_\nu |\langle i|\nu\rangle|^2 e^{i\varepsilon_\nu t}f(\varepsilon_\nu)\right)^2+\left(\sum_\nu |\langle i|\nu\rangle|^2 f(\varepsilon_\nu)\right)^2 -\sum_\nu |\langle i|\nu\rangle|^2 f(\varepsilon_\nu)+\frac{1}{4}. \tag{3.3}$$

Here $|\nu\rangle$ is a one-fermion eigenstate of $\tilde{H}$ Eq. (2.1) with energy ε_ν and $f(x)=[\exp(\beta x)+1]^{-1}$ is the Fermi function. For $J'>J_c=1$ the presence of a localized impurity state with large $|\langle i|\nu\rangle|^2$ and with ε_ν outside the continuum yields a harmonically oscillating nondecaying contribution to $\langle S_i^z(t)S_i^z\rangle$. Similar contributions are contained in every element of the Pfaffian for $\langle S_i^x(t)S_i^x\rangle$, but not in that correlation itself (see Fig. 1, inset). The reason probably is a cancellation of terms due to the multiplications and additions inherent in the definition of the Pfaffian. The time scale introduced by the discrete energy value (3.2) is reflected in the oscillations of $|\langle S^x_{N/2}(t)S^x_{N/2}\rangle|$ (Fig. 1, inset). Similar behavior is found for $T>0$ and will be discussed in the next subsection.

For $J'\leqslant 1$ the time-dependent term in Eq. (3.3) is proportional to

$$\left(\int_{-1}^{1} d\varepsilon (1-\varepsilon^2)^{-1/2} e^{i\varepsilon t} f(\varepsilon)|\langle i|\varepsilon\rangle|^2\right)^2, \tag{3.4}$$

where $\langle i|\varepsilon\rangle$ corresponds to $\langle i|\nu\rangle$ in Eq. (3.3) and the inverse square root factor is the one-particle density of states of the dispersion (2.4) (which still describes the energy eigenvalues, only with slightly displaced k values for $J'\neq 1$). For $J'=1$, $|\langle i|\varepsilon\rangle|^2$ does not depend on ε, the inverse square-root singularities at the band edges $\varepsilon\to\pm 1$ lead to a $t^{-1/2}$ asymptotic behavior of the integral, and to a t^{-1} behavior of $\langle S_i^z(t)S_i^z\rangle$. For $J'<1$ the amplitude of the one-particle eigenstate with energy ε at the impurity site is

$$|\langle i|\varepsilon\rangle|^2=\left[J'^2+\frac{(1-J'^2)^2}{J'^2}\,\frac{\varepsilon^2}{1-\varepsilon^2}\right]^{-1} \tag{3.5}$$

(apart from weakly ε-dependent normalization factors). This changes the band-edge singularities in Eq. (3.4) from $(1-\varepsilon^2)^{-1/2}$ to $(1-\varepsilon^2)^{1/2}$, so that the integral contains a $t^{-3/2}$ term. Consequently, $\langle S_i^z(t)S_i^z\rangle$ contains a t^{-3} term which dominates for $T>0$ (see next subsection). At $T=0$, however, the leading term is proportional to t^{-2} due to the discontinuity of the Fermi function in Eq. (3.4).

We have also studied the x and z autocorrelations of nearest and next-nearest neighbors of the impurity spin $i=N/2$. For weak impurity coupling ($J'\lesssim 0.2$) the x correlation functions of spins $i=N/2+1$ and $i=N/2+2$ show weak oscillations superimposed on a $t^{-1/2}$ decay masked by strong finite-size effects. The z correlations (for $J'<1$) show stronger oscillations. Their decay looks roughly like a power law with an exponent between -2 and -3.

B. $T>0$

Whereas at $T=0$ only power-law decay is observed, exponential decay[29] becomes possible at finite T. Figure 3 shows x and z impurity spin autocorrelations at $J'=0.3$ for several decades in T. There are two well-defined temperature regimes with a crossover between them. Within each regime the correlation functions do not change qualitatively: note that several of the curves in Fig. 3 coincide. The x autocorrelation in the high-T regime shows exponential decay which persists over the entire time range during which the the results are free of finite-size effects. The z autocorrelation decays exponentially at first and later crosses over to the t^{-3} law derived above, with superimposed oscillations which are absent in the low-temperature regime. The appearance of oscillations (if only of small amplitude) in $\langle S_i^z(t)S_i^z\rangle$ at high T is reminiscent of the phenomena recently reported[25] for a two-level system coupled to a spin bath. In that system, a persistence of oscillations up to infinite T could be observed.

Figure 4 shows $|\langle S^x_{N/2}(t)S^x_{N/2}\rangle|$ at $T=10^5$ for impurity coupling $0.1\leqslant J'\leqslant 1$ in a $N=128$ chain. As autocorrelations at $T=\infty$ are real even power series in t, all curves start with zero slope at $t=0$, but then (with the exception of $J'=1$) bend over to a nearly perfect exponential decay. The inset shows the decay rate of that exponential decay as fitted to the data in the main plot. Also shown is the decay rate deter-

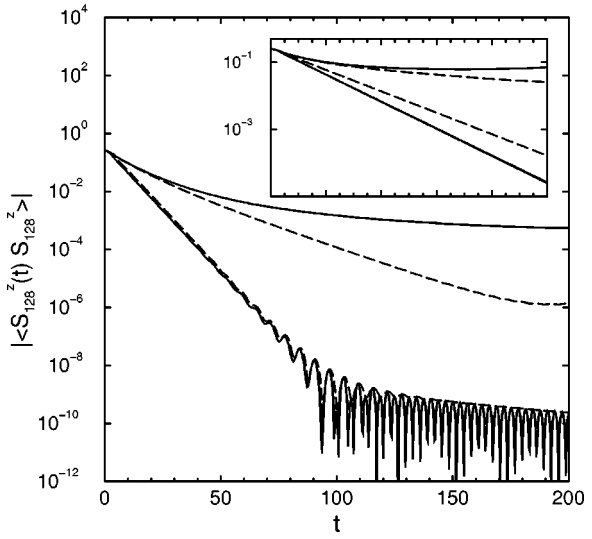

FIG. 3. Crossover between the regimes of high temperature (lower set of curves) and low temperature (upper set of curves). Main plot: Impurity spin-autocorrelation function $|\langle S^z_{N/2}(t)S^z_{N/2}\rangle|$ ($N=256$) with impurity coupling $J'=0.3$ for temperatures $T=10^6$, 10^4, 10^2, 10^0, 10^{-1}, 10^{-2}, 10^{-3}, 10^{-4}, 10^{-5}, and 10^{-6} (bottom to top). The curves for $T=10^{-1}$ and 10^{-2} are long-dashed, all others are solid. Note that several curves coincide on the scale of the figure. Inset: same as the main plot, for $|\langle S^x_{N/2}(t)S^x_{N/2}\rangle|$ ($N=128$); time range is $0<t<100$.

mined from data for $T=1$, and for $J'>1$. Differences between $T=1$ and $T=\infty$ are to be expected and are indeed visible in the behavior of the decay rate close to $J'=1$: For finite T the x autocorrelation function of a homogeneous chain $J_i\equiv 1$ is known[20,21] to decay exponentially with a finite T-dependent decay rate, whereas for infinite T the decay is

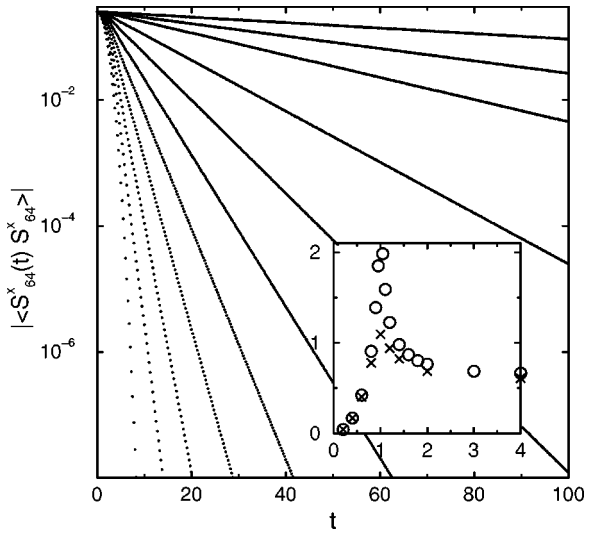

FIG. 4. Exponential decay of the bulk impurity spin x autocorrelation function at high temperature. Main plot: $|\langle S^x_{N/2}(t)S^x_{N/2}\rangle|$ ($N=128$) at $T=10^5$ for impurity couplings $J'=0.1$, 0.15, 0.2, 0.3, 0.4, 0.5, 0.6, 0.7, 0.8, 0.9, and 1 (top to bottom). Inset: Exponential decay rates determined from the data shown in the main plot, and from analogous data for $J'>1$ and for $T=1$. The circles are $T=10^5$ data, the crosses are $T=1$ data. Note the pronounced differences near $J'=1$, where the infinite-T decay rate diverges.

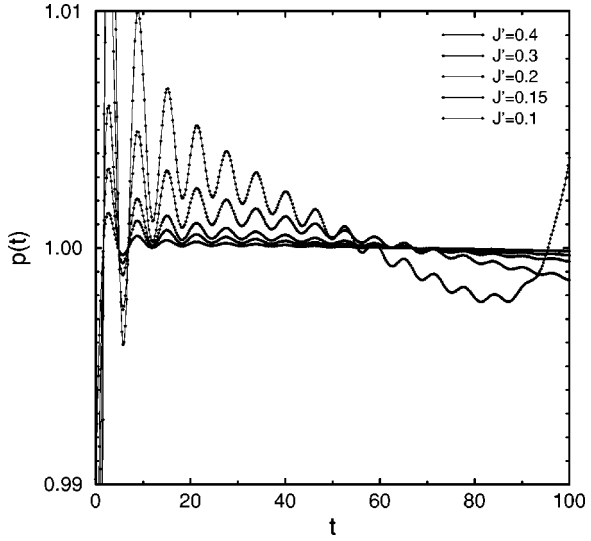

FIG. 5. Precision of the exponential decay of the high-temperature bulk impurity spin correlation function. Shown is the precision function $p(t)$ Eq. (3.6) for the data for $J'\leqslant 0.4$ from the main plot of Fig. 4.

Gaussian.[8,9,18] The Gaussian decay corresponds to a divergence of the exponential decay rate which is obvious in the inset of Fig. 4.

For $J'>1$ $|\langle S^x_{N/2}(t)S^x_{N/2}\rangle|$ is no longer (almost) purely exponential, but develops considerable oscillations. The exponential decay rate grows with T, but decreases as J' grows, as shown in the inset of Fig. 4. As in the $T=0$ case the frequency of the oscillations is proportional to ε_0 Eq. (3.2).

In order to obtain a quantitative measure of the precision to which the decay of $|\langle S^x_{N/2}(t)S^x_{N/2}\rangle|$ at $T=10^5$ follows an exponential, we fitted an exponential law $a\exp(-bt)$ to the numerical data for $0<t<100$ and calculated the quantity

$$p(t):=\frac{|\langle S^x_{N/2}(t)S^x_{N/2}\rangle|}{a\exp(-bt)}, \tag{3.6}$$

which should equal unity for a purely exponential decay.

For $J'\leqslant 0.4$, $p(t)$ is shown in Fig. 5. Note that the scale of the figure extends only to a maximum deviation of 1% from purely exponential decay. The general slope in the data is a natural consequence of the intrinsically nonexponential behavior of the correlation function for small t which was mentioned above. The data for $J'\leqslant 0.2$ follow the purely exponential fit to a precision of better than two parts in thousand for $t\geqslant 10$. This rules out the stretched-exponential behavior reported[30] for $J'\leqslant 0.2$ at $T=\infty$ in an approximate study based on extrapolation of truncated continued-fraction expansions. Figure 5 also reveals the presence of tiny oscillations which are invisible on the scale of Fig. 4. The frequency of these oscillations is independent of J', in contrast to the stronger oscillations for $J'>1$ already mentioned above.

The main differences between x and z spin autocorrelation functions were already shown in Fig. 3. Some more detail on the behavior of $|\langle S^z_{N/2}(t)S^z_{N/2}\rangle|$ is presented in Fig. 6. The main plot shows the crossover between the exponential and t^{-3} (with superimposed oscillations) regimes for three small J' values. With growing J' the exponential decay rate grows

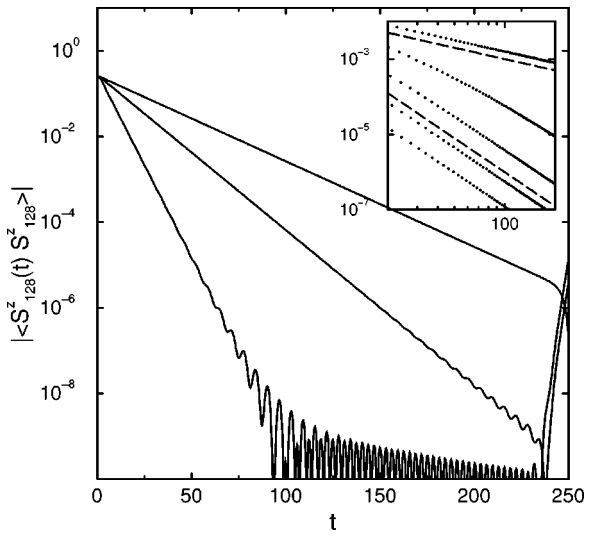

FIG. 6. Initially exponential and asymptotic power-law decay of the bulk impurity z spin autocorrelation function at high temperature. Main plot: $|\langle S^z_{N/2}(t)S^z_{N/2}\rangle|$ ($N=256$) at $T=10^5$ for impurity couplings $J'=0.15$, 0.2, and 0.3 (top to bottom). Note how the exponential regime gets shorter as J' grows. The features in the lower right corner are finite-size effects. Inset: Maxima of $|\langle S^z_{N/2}(t)S^z_{N/2}\rangle|$ for $J'=1$, 0.9, 0.8, 0.7, and 0.6 (top to bottom) and $T\geqslant 20$. The dashed straight lines represent the t^{-1} and t^{-3} power laws.

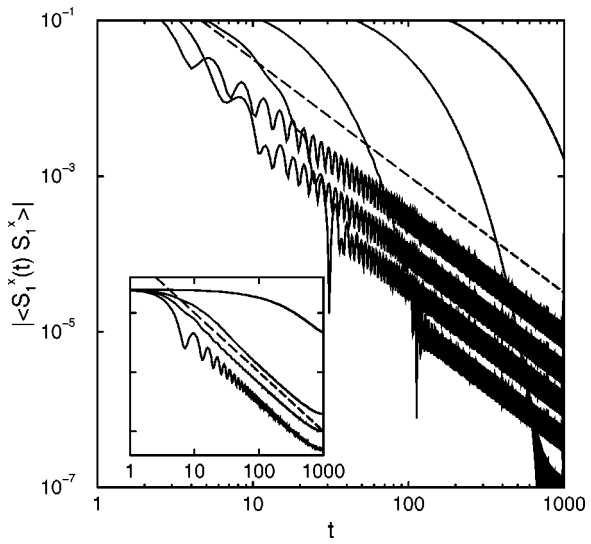

FIG. 7. Boundary spin x autocorrelation function $|\langle S^x_1(t)S^x_1\rangle|$. Main plot: High-temperature regime, $T=1$, $N=512$, and impurity coupling $J'=1$, 0.8, 0.6, 0.4, 0.2, and 0.1 (left to right, according to the point where the curves enter the figure at the upper boundary). The dashed line shows the $t^{-3/2}$ law. Inset: Low-temperature regime, $T=0$, $N=1024$, and $J'=1$, 0.7, 0.5, and 0.1 (bottom to top). The dashed line shows the t^{-1} law.

and the exponential regime shortens in such a way that in the exponential regime $|\langle S^z_{N/2}(t)S^z_{N/2}\rangle|$ is a decreasing function of J' whereas in the power-law regime it is an increasing function of J'. We have deliberately chosen a very long time window in order to illustrate how finite-size effects manifest themselves (for $t\gtrsim 230$). In the inset of Fig. 6 we demonstrate the asymptotic power-law behavior for larger values of J'. The dots represent the maxima of $|\langle S^z_{N/2}(t)S^z_{N/2}\rangle|$, which follow the t^{-3} (for $J'<1$) and t^{-1} (for $J'=1$) laws already discussed. For $J'>1$ the behavior changes to a ''constant with oscillations'' type of asymptotics, similar to the $T=0$ situation shown in the inset of Fig. 2. For $T>0$, however, the amplitude of the oscillations is considerably larger than for $T=0$.

The high-temperature spin autocorrelations of the nearest and next-nearest neighbors to the impurity (for $J'\leqslant 1$) do not show any particularly surprising features. The z correlations do not show exponential decay in the beginning. Instead they oscillate and the maxima of the oscillations display the familiar t^{-3} (for $J'<1$) and t^{-1} (for $J'=1$) laws. The x autocorrelations interpolate smoothly between two known limiting cases. At $J'=1$ the x autocorrelation of the spin $i=N/2+1$ of course is a Gaussian as that of any other bulk spin. At $J'=0$, however, $i=N/2+1$ is the first spin in a semi-infinite homogeneous chain, whose $T=\infty$ autocorrelation function is[19] a combination of Bessel functions with an asymptotic $t^{-3/2}$ decay. Upon reducing J' from 1 to 0, the development of the characteristic Bessel function oscillations (with zeros hardly depending on J') can be nicely observed. Similarly the time range during which the correlation function follows the expected $t^{-3/2}$ decay grows as J' diminishes. The x autocorrelation of $i=N/2+2$ behaves quite similarly, but only a small number of oscillations is visible (in a linear plot) because of the fast ($t^{-9/2}$) asymptotic decay of the known[19] $J'=0$ Bessel function expression.

IV. BOUNDARY IMPURITY

The boundary impurity is defined by Eq. (1.3). Similarly to the case of the bulk impurity discussed in the previous section, the boundary correlation functions show a low-temperature regime and a high-temperature regime, and we restrict our discussion to the values $T=0$ and $T=1$ which represent these two regimes.

It suffices to discuss the impurity spin x autocorrelation function $\langle S^x_1(t)S^x_1\rangle$, because

$$2\langle S^x_1(t)S^x_1\rangle=\sum_\nu |\langle 1|\nu\rangle|^2 e^{i\varepsilon_\nu t} f(\varepsilon_\nu), \tag{4.1}$$

that is, the square root of the time-dependent part of $\langle S^z_1(t)S^z_1\rangle$ [see Eq. (3.3)]. The presence of an isolated impurity state for $J'>J_c=\sqrt{2}$ (compare Sec. II) should be visible in the dynamic correlation functions. In fact, the asymptotic behavior of $\langle S^x_1(t)S^x_1\rangle$ displays a crossover similar to the one shown in the inset of Fig. 2: for all T the long-time behavior is a power law for $J'<\sqrt{2}$ and a constant for $J'>\sqrt{2}$, with additional oscillations in both regimes.

Figure 7 shows $|\langle S^x_1(t)S^x_1\rangle|$ for impurity coupling $J'\leqslant 1$. For $T=1$ we observe an initially exponential decay followed by a power law. The exponential decay rate grows with J'. The duration of the initial exponential phase decreases with growing J' in such a way that in the subsequent power-law regime the correlation function is an increasing function of J'. This behavior is [not unexpectedly, compare Eq. (4.1)] similar to that of the bulk impurity z autocorrelation discussed in Sec. III B, however, the asymptotic power law is a different one, namely the $t^{-3/2}$ law known for the boundary

spin[19] of the homogeneous semi-infinite chain at infinite T, and for a range of boundary spins[21] of the same system at finite T.

At this point, the early analytical study by Tjon[5] should be mentioned. In the limit of sufficiently small J' Tjon found an asymptotically exponential decay $\sim e^{-t/\tau}$ for $\langle S_1^x(t)S_1^x\rangle$, with decay rate $\tau^{-1}=\frac{1}{2}J'^2$. Indeed, our numerical data show that during the exponential regime mentioned above, the decay rate is quite precisely equal to $\frac{1}{2}J'^2$ for $J'\lesssim 0.2$, and a bit larger for larger J'. However, we also observe numerically (and explain analytically, see below) a crossover from exponential to power-law behavior. The duration of the exponential regime grows ($\sim J'^{-2}$) as J' becomes weak and thus our numerical results for arbitrary J' connect smoothly to Tjon's analytical result restricted to the weak-coupling limit.

The inset of Fig. 7 shows $|\langle S_1^x(t)S_1^x\rangle|$ for $T=0$ and $J'<1$. After a very slow initial decay (slower for smaller J') the curves eventually all bend over to show a t^{-1} asymptotic decay developing some oscillations as J' approaches unity. The t^{-1} decay at $T=0$ is again a well-known feature[10] of the homogeneous semi-infinite chain.

The asymptotic power laws may be understood from the properties of the analytic solution of the boundary impurity (one-particle) problem, along the lines of the discussion in Sec. III A. According to Eq. (4.1), $|\langle S_1^x(t)S_1^x\rangle|$ for $J'<\sqrt{2}$ is given by an integral analogous to the one in Eq. (3.4). The analytic solution shows that the wave function factor in the integral, $\langle 1|\varepsilon\rangle\sim\sin k$, where $\varepsilon=-\cos k$. This leads to a band-edge singularity $\sim(1-\varepsilon)^{1/2}$ in the integrand, and a $t^{-3/2}$ asymptotic behavior of the integral. At $T=0$ the $t^{-3/2}$ contribution is dominated by the t^{-1} contribution from the discontinuity of the Fermi function.

V. SUMMARY AND CONCLUSIONS

The dynamic spin correlation functions associated with isolated impurities in a $S=\frac{1}{2}$ XX chain show a rich behavior depending on the temperature, the impurity coupling strength J', the spin component ($\alpha=x,z$) under consideration, and on the position of the impurity spin in the chain. Regimes of low and high T, with qualitatively different behavior of the correlations may be distinguished. We have summarized the asymptotic behavior of the bulk x and z spin autocorrelations in these two T regimes in Table I. The basic features of the boundary correlations may also be obtained from Table I by observing that (i) the z autocorrelation does not change fundamentally between bulk and boundary and (ii) at the boundary the x autocorrelation behaves as the square root of the z autocorrelation.

TABLE I. Asymptotic decay of the bulk x and z autocorrelation functions. Additional oscillations of varying strength are present in all cases.

	Low T	High T
x	$t^{-1/2}$	$e^{-t/\tau}$
$z, J'<1$	t^{-2}	t^{-3} (after initial $e^{-t/\tau}$)
$z, J'>1$	t^{0}	t^{0}

As mentioned in the Introduction, the present model may be interpreted as a single two-level system in contact with a large bath. The influence of the nature of the bath degrees of freedom on the type of decay of the two-level system was addressed recently[25] for a spin bath constructed in a way to resemble closely the standard[23] harmonic oscillator bath. The following results were found. At $T=0$ the spin bath leads to damped oscillations in the two-level system, as does the oscillator bath. However, at high T, the oscillations vanish for the oscillator bath but persist for the spin bath.

Without going into any detailed comparison between the spin bath employed in Ref. 25 and the XX chain studied here, we would like to point out the existence of similar oscillation phenomena at high T in the present system. Figure 3 (main plot) shows how the bulk impurity spin z autocorrelation function develops oscillations as temperature *increases*. Whether these oscillations can be unambiguously assigned to either the impurity or the bath, and what happens for systems interpolating between the present one and that of Ref. 25, remains to be seen in further studies.

ACKNOWLEDGMENTS

We are grateful to Professor Gerhard Müller (University of Rhode Island) for helpful comments and suggestions.

[1] E. Lieb, T. Schultz, and D. Mattis, Ann. Phys. (N.Y.) **16**, 407 (1961).
[2] S. Katsura, Phys. Rev. **127**, 1508 (1962).
[3] T. Niemeijer, Physica (Amsterdam) **36**, 377 (1967).
[4] S. Katsura, T. Horiguchi, and M. Suzuki, Physica (Amsterdam) **46**, 67 (1970).
[5] J. A. Tjon, Phys. Rev. B **2**, 2411 (1970).
[6] B. M. McCoy, E. Barouch, and D. B. Abraham, Phys. Rev. A **4**, 2331 (1971).
[7] A. Sur, D. Jasnow, and I. J. Lowe, Phys. Rev. B **12**, 3845 (1975).
[8] U. Brandt and K. Jacoby, Z. Phys. B **25**, 181 (1976).
[9] H. W. Capel and J. H. H. Perk, Physica A **87**, 211 (1977).
[10] W. Pesch and H. J. Mikeska, Z. Phys. B **30**, 177 (1978).
[11] H. G. Vaidya and C. A. Tracy, Physica A **92**, 1 (1978).
[12] L. L. Gonçalves and H. B. Cruz, J. Magn. Magn. Mater. **15-18**, 1067 (1980).
[13] H. B. Cruz and L. L. Gonçalves, J. Phys. C **14**, 2785 (1981).
[14] B. M. McCoy, J. H. H. Perk, and R. E. Shrock, Nucl. Phys. B **220** [FS8], 35 (1983).
[15] B. M. McCoy, J. H. H. Perk, and R. E. Shrock, Nucl. Phys. B **220** [FS8], 269 (1983).
[16] G. Müller and R. E. Shrock, Phys. Rev. B **29**, 288 (1984).
[17] J. H. Taylor and G. Müller, Physica A **130**, 1 (1985).
[18] J. Florencio and M. H. Lee, Phys. Rev. B **35**, 1835 (1987).
[19] J. Stolze, V. Viswanath, and G. Müller, Z. Phys. B **89**, 45 (1992).
[20] A. R. Its, A. G. Izergin, V. E. Korepin, and N. A. Slavnov, Phys.

Rev. Lett. **70**, 1704 (1993).
[21] J. Stolze, A. Nöppert, and G. Müller, Phys. Rev. B **52**, 4319 (1995).
[22] A. J. Leggett *et al.*, Rev. Mod. Phys. **59**, 1 (1987).
[23] U. Weiss, *Quantum Dissipative Systems* (World Scientific, Singapore, 1993).
[24] P. Hänggi, P. Talkner, and M. Borkovec, Rev. Mod. Phys. **62**, 251 (1990).
[25] J. Shao and P. Hänggi, Phys. Rev. Lett. **81**, 5710 (1998).
[26] W. H. Press, S. A. Teukolsky, W. T. Vetterling, and B. P. Flannery, *Numerical Recipes in FORTRAN: the Art of Scientific Computing* (Cambridge University Press, Cambridge, 1992).
[27] The properties of Pfaffians, close relatives of determinants, are discussed in Ref. 31, the explicit formula for $\langle S_i^x(t)S_j^x\rangle$ is given in Ref. 21.
[28] For the bulk impurity (1.4) a system with $N-1$ sites should be considered for symmetry.
[29] The real (imaginary) part of the autocorrelation function of a Hermitian operator is an even (odd) function of time, hence purely exponential decay is not possible. A theorem ruling out purely exponential decay for a broad class of systems was stated by Lee (Ref. 32). In the present paper, we always refer to an (approximately) exponential decay in a time range limited for general reasons at short times and by finite-size effects at long times.
[30] S. Sen and T. D. Blersch, Physica A **253**, 178 (1998).
[31] H. S. Green and C. A. Hurst, *Order-Disorder Phenomena* (Wiley-Interscience, London, 1964).
[32] M. H. Lee, Phys. Rev. Lett. **51**, 1227 (1983).